Control Strategies for a Unified Power Quality Conditioner with Hybrid Energy Storage in a Low-Voltage Distribution Network

Jose M. Piedra
Engineering Dept.
Gesinne S.L.
Gijón, Spain
josemanuel@gesinne.com

Pablo García
Electrical Engineering Dept.
University of Oviedo
Gijón, Spain
garciafpablo@uniovi.es

Ramy Georgious
Electrical Engineering Dept.
University of Oviedo
Gijón, Spain
georgiousramy@uniovi.es

Miguel Crespo
R&D Department
Cegasa Energía S.L.U.
Miñano, Spain
mcrespo@cegasa.com

***Abstract*—This paper proposes the design, analysis and control of a Unified Power Quality Conditioner with embedded hybrid energy storage, based on supercapacitors and Li-ion batteries for power condition in distribution grids. The proposed system is able to compensate voltage sags and swells, current unbalances as well as operation in grid-forming mode when required. The paper is focused on the complete system design, including the power stage, energy storage and control system. System operation is assessed by using a real profile obtained from a power meter installed in an industrial installation.**

***Index Terms*—UPQC, Hybrid Energy Storage, Distribution Networks, Power Quality**

I. Introduction

Power quality events affecting the distribution grid are a major concern for modern power systems [1]. Active compensation can be achieved both by series or/and parallel (shunt) connection [2]. The combination of both is known as Unified Power Quality Conditioner (UPQC), which is close related to the Unified Power Flow Controller (UPFC) used in transmission systems [3], [4]. The basic UPQC configuration uses a shunt connected device to keep the dc-link constant as well as to compensate unbalances and harmonics currents demanded by the load and a series device, in back-to-back configuration with the shunt, to control the load-side voltage, thus reducing the effect of voltage sags and swells [3]. The incorporation of energy storage systems (ess) into the UPQC triggers new capabilities for these devices: 1) stiffer dc-link even with large variations in the AC voltage, 2) wide voltage control variation, including support of black-start operation and 3) operation in the 4-quadrants independently of the grid [5]–[9]. Different technologies have been used for the energy storage integration. However, Li-ion batteries and supercapacitors are among the most popular choices [6], [7], [10].

Operation of UPQC devices for voltage compensation can be implemented by injecting a series voltage in: 1) phase with the line current (UPQC-P), 2) orthogonal voltage to the line current (UPQC-Q) or a combination of both (UPQC-S) [3]. The first alternative is the more effective in terms of voltage compensation, allowing both for compensating sags and swells. However, it requires an increased source current while compensating that in turn could cause further voltage drops in weak grids. The second, only requires reactive power exchange. However, it needs a larger voltage injection for the compensation and can not be used for the compensation of voltage swells. The third is a combination of the first two, in which the voltage is injected with a given angle with respect to the line current. It adds control complexity and still can not operate when the grid is not present. In this paper, the incorporation of a hybrid energy storage system, based on a Li-ion battery and supercapacitor modules, into the UPQC topology allows for the active power compensation (UPCQ-P) with a reduced impact on the grid current, thus improving the system controllability and the dc-link stiffness. Besides that, the proposed system can work in grid-generation mode. The proposed power converter is shown in Fig. 1. As it can be seen, the ac interface is built by a 4-leg architecture, so neutral current and voltage can be actively controlled.

This paper is structured as follows. In Section II, the system description, including all the parameters used for the design as well as the detailed schematic with the power converter topology is presented. In Section III, the control system design for the shunt, series and energy storage converters is developed. In Section V, simulation results for the system evaluation are included. Finally, the main conclusions of the paper are summarized in Section VI.

II. System description and power converter design

The proposed power converter is based on a shunt-series connection with two dc/dc synchronous power converters for the integration of the energy storage elements. The schematic of the system, as well as the photos for the prototype currently being built, are shown in Fig. 1 and the relevant parameters for the different elements are listed in Table I.

The present work has been partially supported by the European Union's H2020 Research and Innovation programme under Grant Agreement No 864459 (UE-19-TALENT-864459) and the Ministry of Science, Innovation and Universities by the Industrial Doctorates programme reference DIN2018-009853B98667264.

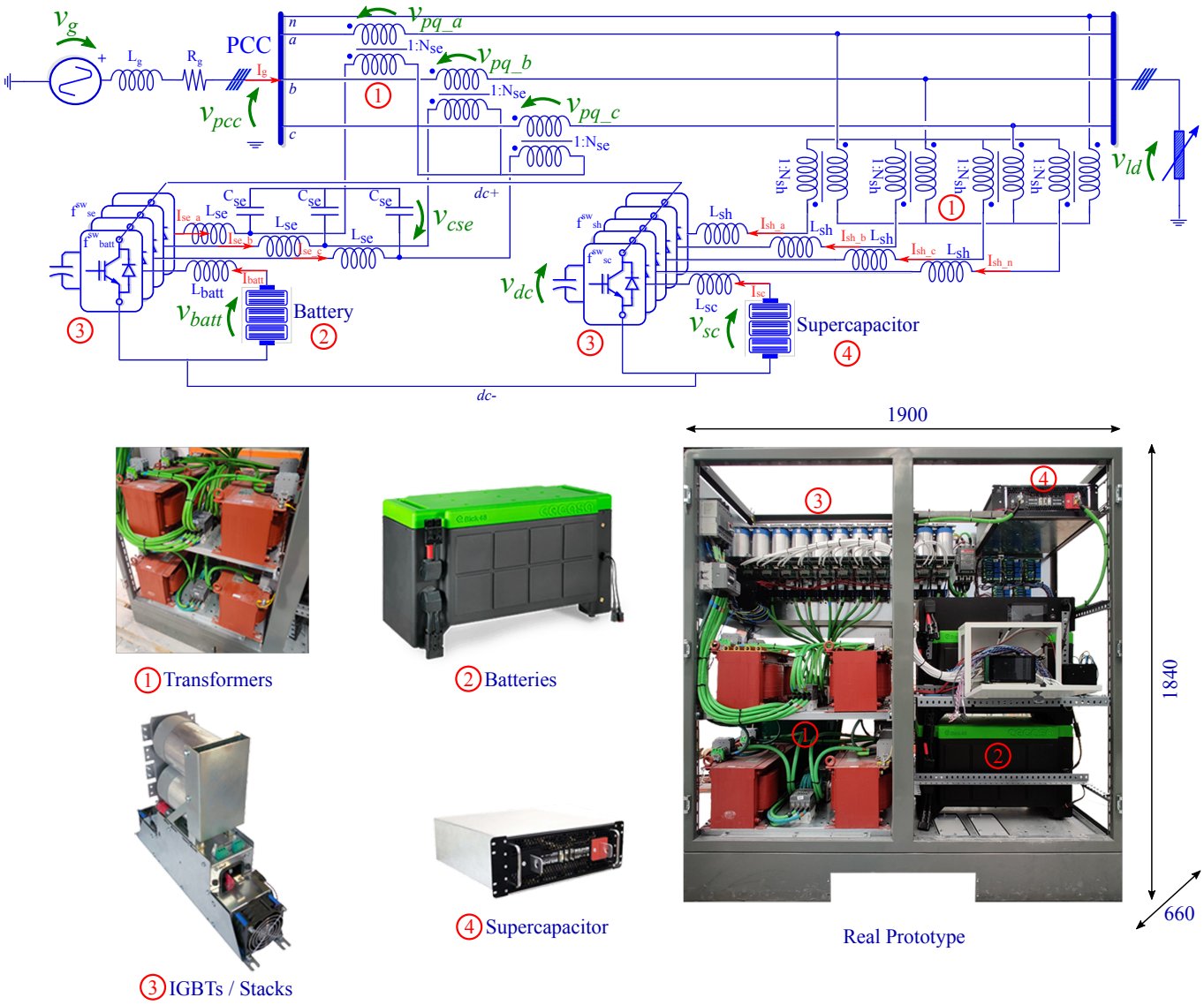

Fig. 1. Schematic for the proposed UPQC-ESS device and details for the prototype under construction.

A. System description

The connection of the proposed compensator to the grid is shown in Fig. 1. In there, it can be seen the connection to the grid point of common coupling (PCC) and the system load. In this paper, the grid is emulated by a series impedance with an ideal voltage source. The series impedance models the line according to the parameters shown in Table I. Four quadrants constant power loads are considered for the sake of generalization.

As discussed in the literature [4], the UPQC connection can be done in two different configurations: 1) shunt connected to the PCC and series following before the load and 2) series at the PCC and shunt downstream. In this paper, configuration 2 has been chosen in which first the series compensation is achieved and after the shunt converter can be dedicated to reactive power and harmonic compensation. The fundamental advantage of this configuration is that the series compensation allows for obtaining a balanced nearly-constant voltage at the shunt and load connection points, thus easing the shunt synchronization and operation. It shall be remarked that, during the black-start operation, the shunt is used for the grid generation while the series converter can be either bypassed or operated with a zero voltage reference.

B. Power converter design

For the power converter design, modularity has played a critical role. Considering the system shall be scaled to different power/energy levels, selection for the power electronics and ess components has been done considering the scalability of

TABLE I
SYSTEM AND CONTROL PARAMETERS.

Parameter	Value	Parameter	Value	Parameter	Value	Parameter	Value
L_{se}	97.2 μH	L_{sh}	0.55 mH	L_{batt}/L_{sc}	0.8 mH	C_{dc}	8.4 mF
C_{se}	1.38 mF	C_{sh}	10.0 μF				
N_{se}	3	N_{sh}	3	$V_{batt}^{nom}/V_{sc}^{nom}$	96/102 V	V_{dc}^{nom}	250 V
$Cvse$ ω_n	50 Hz	$Cish$ ω_n	500 Hz	$Ciess$ ω_n	500 Hz	$Cvdc$ ω_n	50 Hz
$Cvse$ ξ	1	$Cish$ ξ	$\sqrt{2}/2$	$Ciess$ ξ	$\sqrt{2}/2$	$Cvdc$ ξ	1
f_{se}^{sw}	10 kHz	f_{sh}^{sw}	10 kHz	$f_{batt}^{sw}/f_{sc}^{sw}$	10 kHz		
V_g^{ph}	400 V	X/R	0.32	L_{pu}	$0.2\frac{\mu H}{m}$	L_g	1 mH
				R_{pu}	$0.2\frac{m\Omega}{m}$	R_g	1 Ω

TABLE II
SYSTEM COMPONENTS.

Component	Rated Voltage	Rated Current
Power converter stacks MTM-1/2B2IC	400 Vac	180 A
Li-ion battery eBick 180 PRO	48 V	180 A
Supercapacitor module SKELMOD 102 V MODULE	102 V	270 A, 40 deg ΔT

the solution. Details about the system components are listed in Table II. Modular IGBT power stacks from Rectficadores Guasch (9 MTM-1/2B2IC units, 180 A each) have been selected for all the power conversion stages. For the Li-ion battery, two series-connected modules from Cegasa Energía (eBick 180 PRO, 48 V/180 A) are used, whereas a single module from Skeleton is employed for the supercapacitor (SKELMOD 102 V MODULE, 88 F). Rated power for both the shunt and series converter is 100 kW. Regarding the transformer, a $1:3$ ratio has been selected in order to avoid an excessive boost ratio from the dc/dc converter used for the energy storage integration. Single-phase iron core transformers are used. Even though the resulting system is less compact, the independent control of the neutral makes this approach more flexible. AC coupling inductances are also iron-core based. Pictures for the most relevant elements are also shown in Fig. 1.

III. CONTROL SYSTEM DESIGN

The control system has been designed using a classical vector control approach for the shunt and series converters and a non-linear decoupling control for the interface and power sharing of the dc/dc stages used for the interface of the ess. All the enumerated controllers are standard PI in ideal form. Implementation is done in discrete domain using bilinear approximation and synchronous sampling. The system capabilities can be summarized as follows: 1) operation in the 4-quadrants, 2) able to black-start, 3) compensation of system unbalances both in the voltage and load currents. A diagram for the proposed control system is shown in Fig. 2. The implementation of the different control loops is following explained, grouped by power converter: 1) shunt converter, 2) series converter, 3) ess converters.

A. Shunt converter

The shunt converter plays two different roles depending on the operation mode; grid-tied and black-start followed by grid-islanding.

1) Grid-tied operation: When grid-tied, the shunt device is responsible for keeping the dc-link charged as well for compensating for the reactive current demanded by the load. As said before, the control system is implemented using a classical vector control approach, considering the decoupling of feedforward terms derived from the power demands of the series converter. The implemented modulation scheme is a sine-triangle modulation with third harmonic injection, thus being equivalent to basic space vector modulation. The modulator of the 4^{th} leg, connected to the neutral, is commanded to inject the third harmonic, thus avoiding homopolar components due to the power converter modulation to circulate in the neutral connector. The implementation is shown in Fig. 2 a).

2) Black-start operation: In absence of grid due to a fault, the proposed power topology can autonomously provide the energy to the local loads. The shunt-converter is responsible for it, by changing its control mode from STATCOM mode (reactive power compensator) to grid-forming mode. In this operation mode, the dc-link is controlled by the battery dc/dc converter, while the ac voltage is controlled by the shunt converter. The control system implementation is shown in Fig. 2 d). This control mode shall allow a smooth transition to grid-tied operation, by providing a synchronization mechanism between the shunt generated voltage and the grid once the fault is clear. For this, the control system shown in Fig. 3 is proposed. The main idea is to make the synchronization to happen when the vector error between the shunt-side and the grid-side voltage vectors is below a threshold and the next voltage zero-crossing occurs. As shown in the figure, this is implemented by a close-loop method following discussed. The complex error components (magnitude and angle) are calculated and PI controllers are used for the minimization of the error. For the magnitude compensation, the implementation is straightforward and no other considerations need to be

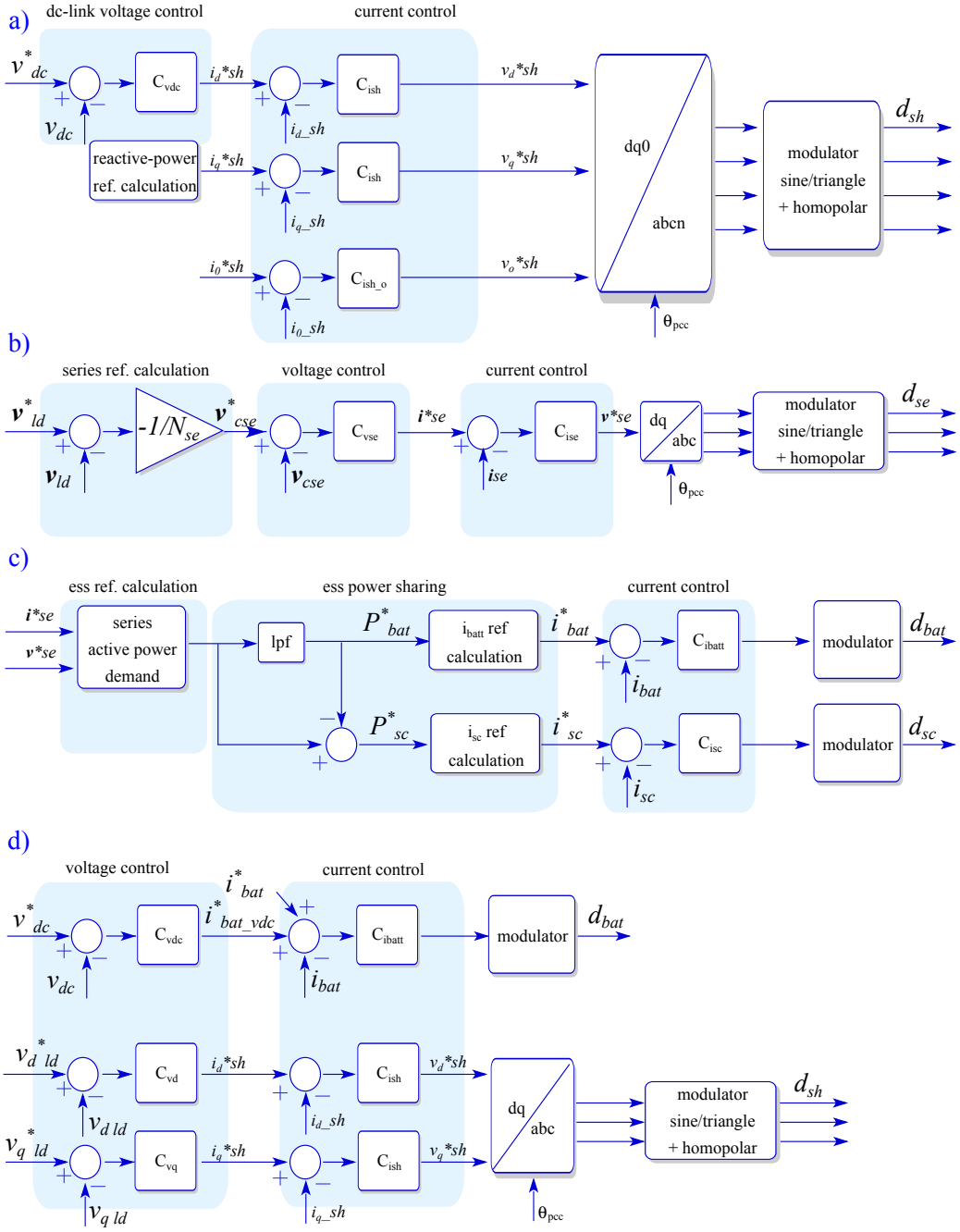

Fig. 2. Control system implementation. a) shunt converter, b) series converter, c) ess converter. d) Control in black-start mode. Bold symbols are used for complex-vector variables representation. Variables as defined in Fig. 1. Controller gains and parameters as given in Table I.

included. However, for the angle error minimization, a detailed explanation is needed. The angle function is wrapped between $[-\pi, \pi]$, what makes direct difference calculation impossible due to the phase jumps. Two strategies can be here used. The first one, which is the simplest solution, it to make a angle unwrap operation before the error computation. This transformation allows to directly calculate the error without any phase jump. However, this strategy could potentially cause resolution problems in the digital implementation due to the variable being unbounded. A second, more interesting approach, is to keep the phase constraint and using the properties of the $\sin$ and $\cos$ functions over the angular difference. When the two vectors are aligned, the $\sin$ of the angle difference will be zero. This makes this signal a good candidate to an error signal to be minimized by the close-loop strategy. However, the same value is reached when the two vectors are in phase opposition (180 deg.). In order to resolve the uncertainty, the $\cos$ function is used as a polarity detection. Considering its value changes from 1 to -1 when the phase error moves from 0 to 180 deg, it could be used as shown in Fig. 3. Even thought this approach

seems quite simple, is needed to remark that the tuning of the two PI controllers used for the phase minimization requires a careful design. As graphically depicted in Fig. 3, the output of the polarity detection compensator is added as a frequency command to the frequency increment commanded by the $\sin$ controller. This makes that this second controller sees the polarity signal as a disturbance, which tries to compensate. If that happens, the wrong alignment could occur. In order to avoid that, a much lower bandwidth is set to the $\sin$ controller than to the polarity one, so the 180 deg jump is successfully achieved when needed.

B. Series converter

The series converter is responsible of load-side voltage regulation. The implementation is shown in Fig. 2 b). As it can be seen, based on the error between the required and real load voltage, a reference for the voltage across the series transformer is generated. From there, using a cascaded vector-control approach, the internal current control and the converter voltage command are successively obtained. Same modulation scheme as in the shunt is used, considering in this case only three legs. As explained in the previous section, when the UPQC works isolated from the grid, the series converter could be either bypass or commanded with zero voltage reference.

C. ESS converter

The ESS converter is built by two independent bidirectional synchronous rectifiers, one for the battery and another for the supercapacitor module. The main objective of the ESS is to compensate for the active power required by the series converter. For that, a power equivalence is established among the series and the two ESS converters. A sharing mechanism consisting on two complementary 1^{st} order low-pass and high-pass filter is used for filtering the power commands to the battery and the supercapacitor respectively. The implementation is shown in Fig 2 c). When the system works isolated from the grid, the dc-link voltage control is implemented using the battery-side converter. The proposed control architecture is shown in Fig. 2 d).

IV. Dynamic model

The system dynamics are accounted considering the different state variables, according to the main system schema shown in Fig. 1. In there, the following variables can be easily seen at the different conversion stages.

1) dc/ac Shunt converter: The power conversion includes, considering the dc-link capacitor to be part of this stage, two states $x_{sh} = [v_{dc}, i_{sh}]$.

2) dc/ac Series converter: The series converter state variables are determined by its output filter, which has a LC structure; $x_{se} = [i_{se}, v_{cse}]$.

3) dc/dc Battery converter: The battery connection is performed by a synchronous rectifier converter, only having an inductor filter; $x_{batt} = [i_{batt}]$.

4) dc/dc Supercapacitor converter: The Supercapacitor conversion scheme is the same than the one used for the battery; $x_{sc} = [i_{sc}]$.

Additionally to the converter-related state variables, the grid input current is also defined as an state variable $x_g = [i_g]$. The manipulated input variable at all the conversion stages is named as the corresponding duty cycle $[d_{sh}, d_{se}, d_{bat}, d_{sc}]$. It shall be remarked that for the multiphase converters, i.e. shunt and series, the input variables are considered vectors with the same dimensions than the number of controlled phases (4 for the shunt and 3 for the series). The proposed model could also be extended to include the transformers dynamics, considering the leakage inductance. However, being the transformer series connected to each of the dc/ac converter output filters, the overall dynamics are generally dominated by the filter impedance and thus are here neglected. The grid voltage, v_g, battery voltage, v_{bat}, and supercpacitor voltage, v_{sc}, are modelled as external inputs. The system output variable, and the one to be controlled, is the voltage at the pcc v_{pcc}. For the base case, when the UPQC is not installed, the pcc voltage matches the load voltage $v_{pcc} = v_{ld}$. In here it shall be remarked the ac variables are represented by the corresponding complex-vectors.

The proposed dynamic model is shown in Fig. 4. Two different colors are used for representing the original uncontrolled load (grey) and the paths added by the UPQC (blue). From the block diagram, it is clear how the shunt converter could be used for the filtering of the load current by controlling the i_{sh} current and the series converter to compensate for the load voltage variations by the manipulation of the v_{pq} voltage. The modelling also captures the use of the energy storage system and its role in the sharing of the dc-link voltage. The dc-link voltage is affected by the current sources connected to it; the battery current, i_{bat}, the supercapacitor current, i_{sc}, as well as the dc-link-referred shunt converter current, i_{sh}^{dc} and series one i_{se}^{dc}. The signs clearly shown the energy balance, being the series converter a energy-sink port and the shunt converter a energy-source. In the absence of the energy storage, the demanded energy from the series converter has to be supplied from the shunt.

As it can be seen, is a non-linear average model that can be easily used for the tuning of the proposed control system. The cascade-based control architecture is designed so each of the controllers tackles its own state dynamics. Non-linearities are decoupled as shown in the control system implementation.

V. Simulation Results

For the initial evaluation, a switching model has been implemented in PLECS. The simulation results are shown in Fig. 5. Real grid voltage profiles have been obtained with a power analyzer installed in the PCC of a posible final user of the proposed system. The data was obtained with a 10 kHz sampling frequency. The most relevant grid events have been used for the generation of the test profile. Additionally, an active load working in the four quadrants has been considered to evaluate the system disturbance rejection capabilities as

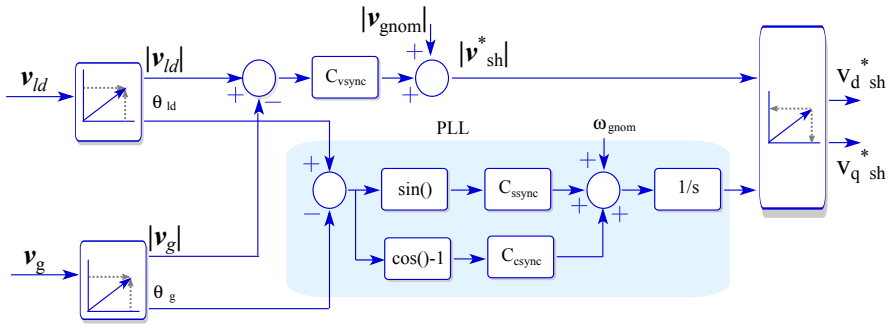

Fig. 3. Proposed scheme for the grid synchronization from the black-start to the grid-connected mode. Bandwidth for the C_{ssync} and C_{csync} are respectively established as 0.1 Hz and 20 Hz.

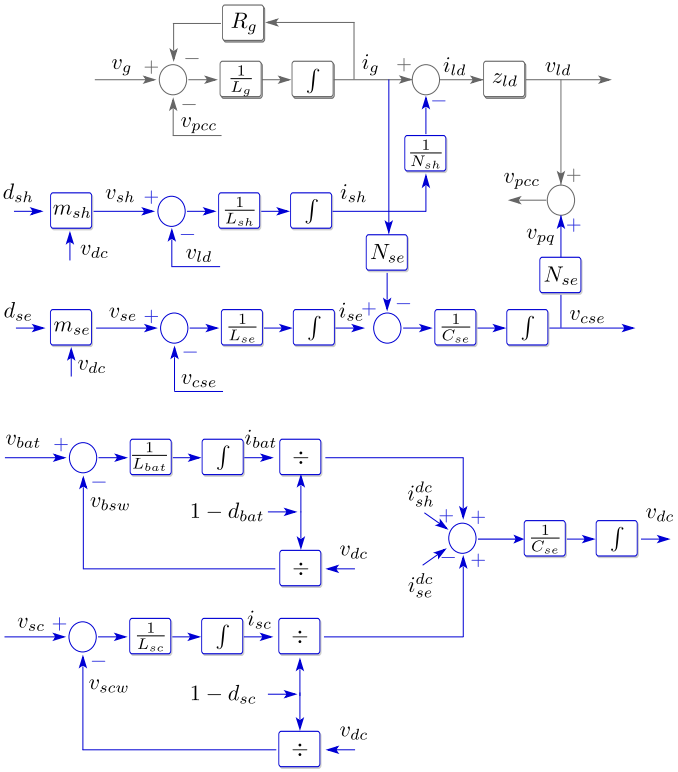

Fig. 4. Dynamic model for the proposed UPQC converter with energy storage. Variable names as represented in Fig. 1. i_{sh}^{dc} and i_{se}^{dc} are referred to the dc-side shunt and series converter current calculated from the i_{sh} and i_{se} ac-side current vectors using the converter switching function.

well as the reactive power compensation. The following load changes are considered: at t=0.5 s, a 10 kW active load is connected. At t=0.6 s, the same load is applied in generation mode. At t=0.7 s, -5 kVA of reactive power are added. The load is applied as an step-wise function, filtered by a 2^{nd} low-pass filter, 1 kHz bandwidth. The simulation test is described as follows:

1) The converter starts in grid-connection mode. At t=0.1 s, the shunt device charges the dc-link to the rated value (250 V). The series converter has the bypass enabled and the ess converters are disconnected.
2) The ess converters are enabled at t=0.3 s. As it can be seen, the power sharing between the battery and supercapacitor meet the active power commanded by the series converter (Fig. 5h).
3) At t=0.4 s, the series converter bypass is opened and the control system is enableb. The load-voltage is controlled to the desired voltage reference (340 V) (see Fig. 5b).
4) At t=0.7 s, a change in the reactive power demmanded by the load is commanded. The shunt reactive power compensator is disabled.
5) At t=0.1.05 s, the reactive power compensator is enabled. The reactive power is thus controlled by the shunt converter, while the grid reactive current drops to zero (see Fig. 5d and Fig. 5f).

This operation modes allows to determine that the power converter can effectively compensate for different kind of loads and grid-voltage variarions.

VI. Conclusion

This paper has demonstrated the feasible operation of a UPQC in the 4-quadrants. A detailed dynamic model and the control system design have been also included. The proposed system has been evaluated by simulation results, in which the different considered control modes are evaluated. Description of the converter assembly, including references for all the main components, as well as design specifications has been as well included.

References

[1] R. Dugan, M. McGranaghan, S. Santoso, and H. Beaty, *Electrical Power System Quality*. McGraw-Hill, New York, 72-79, 1996.
[2] H. Akagi, "Trends in active power line conditioners," *IEEE Transactions on Power Electronics*, vol. 9, no. 3, pp. 263–268, May 1994.
[3] V. Khadkikar, "Enhancing electric power quality using upqc: A comprehensive overview," *IEEE Transactions on Power Electronics*, vol. 27, no. 5, pp. 2284–2297, May 2012.
[4] M. Farhadi-Kangarlu, E. Babaei, and F. Blaabjerg, "A comprehensive review of dynamic voltage restorers," *International Journal of Electrical Power and Energy Systems*, vol. 92, pp. 136 – 155, 2017. [Online]. Available: http://www.sciencedirect.com/science/article/pii/S0142061516328149
[5] Z. Liu, S. Miao, Z. Fan, K. Chao, and Y. Kang, "Coordinated power allocation and robust dc voltage control of upqc with energy storage unit during source voltage sag," in *2018 IEEE Power Energy Society General Meeting (PESGM)*, Aug 2018, pp. 1–5.

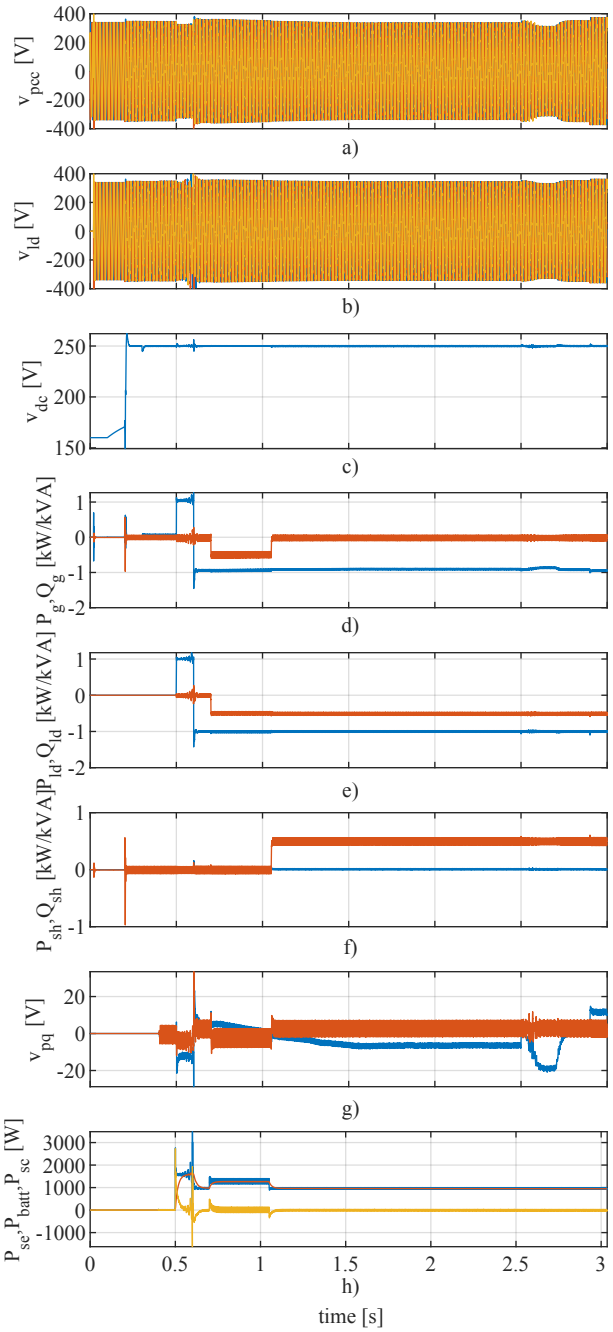

Fig. 5. Simulation results. From top to bottom and left to right: a) voltage at the pcc; b) load voltage; c) dc-link voltage; d) active (blue) and reactive (red) grid power; e) active (blue) and reactive (red) load power; f) active (blue) and reactive (red) shunt power; g) series voltage injection in synchronous reference frame: d-axis (blue), q-axis (red); h) ess power: ess power reference (blue), battery power (red), supercapacitor power (yellow).

[6] D. Somayajula and M. L. Crow, "An integrated dynamic voltage restorer-ultracapacitor design for improving power quality of the distribution grid," *IEEE Transactions on Sustainable Energy*, vol. 6, no. 2, pp. 616–624, April 2015.

[7] N. M. Ismail and M. K. Mishra, "Control and operation of unified power quality conditioner with battery-ultracapacitor energy storage system," in *2014 IEEE International Conference on Power Electronics, Drives and Energy Systems (PEDES)*, Dec 2014, pp. 1–6.

[8] L. Han, X. Feng, X. Che, T. Zhang, and T. Wei, "Unified power quality conditioner based on fast energy storage," in *2014 IEEE 8th International Power Engineering and Optimization Conference (PEOCO2014)*, March 2014, pp. 423–428.

[9] A. Moghadasi, S. M. Torabi, and M. Salehifar, "Performance evaluation of unified power quality conditioner with smes," in *2010 First Power Quality Conferance*, Sep. 2010, pp. 1–6.

[10] P. Jayaprakash, B. Singh, D. P. Kothari, A. Chandra, and K. Al-Haddad, "Control of reduced-rating dynamic voltage restorer with a battery energy storage system," *IEEE Transactions on Industry Applications*, vol. 50, no. 2, pp. 1295–1303, March 2014.